



Gastrointestinal Emergency in Neonates and Infants: A Pictorial Essay

Gayoung Choi¹, Bo-Kyung Je¹, Yu Jin Kim²

¹Department of Radiology, Korea University Ansan Hospital, Ansan, Korea; ²Department of Radiology, Samsung Medical Center, Sungkyunkwan University School of Medicine, Seoul, Korea

Gastrointestinal (GI) emergencies in neonates and infants encompass from the beginning to the end of the GI tract. Both congenital and acquired conditions can cause various GI emergencies in neonates and infants. Given the overlapping or nonspecific clinical findings of many different neonatal and infantile GI emergencies and the unique characteristics of this age group, appropriate imaging is key to accurate and timely diagnosis while avoiding unnecessary radiation hazard and medical costs. In this paper, we discuss the radiological findings of essential neonatal and infantile GI emergencies, including esophageal atresia and tracheoesophageal fistula, hypertrophic pyloric stenosis, duodenal atresia, malrotation, midgut volvulus for upper GI emergencies, and jejunoileal atresia, meconium ileus, meconium plug syndrome, meconium peritonitis, Hirschsprung disease, anorectal malformation, necrotizing enterocolitis, and intussusception for lower GI emergencies.

Keywords: *Gastrointestinal emergency; Neonate; Infant; Intestinal atresia; Tracheoesophageal fistula; Midgut volvulus; Meconium plug syndrome; Hirschsprung disease; Anorectal malformation; Necrotizing enterocolitis; Intussusception; Imaging*

INTRODUCTION

Gastrointestinal (GI) emergencies in neonates and infants can occur anywhere from the beginning to the end of the GI tract. While prenatal imaging can be helpful in revealing the underlying causes, postnatal radiologic evaluation with meticulous history taking and physical examination are required to narrow the differential diagnosis, select the proper treatment, and minimize potential mortality and morbidity [1]. In this pictorial essay, we discuss the essential imaging features of neonatal and infantile GI emergencies in two parts: the upper GI and the lower GI.

Received: February 3, 2021 **Revised:** August 29, 2021

Accepted: September 13, 2021

Corresponding author: Bo-Kyung Je, MD, PhD, Department of Radiology, Korea University Ansan Hospital, 123 Jeokgeum-ro, Danwon-gu, Ansan 15355, Korea.

• E-mail: radje@korea.ac.kr

This is an Open Access article distributed under the terms of the Creative Commons Attribution Non-Commercial License (<https://creativecommons.org/licenses/by-nc/4.0>) which permits unrestricted non-commercial use, distribution, and reproduction in any medium, provided the original work is properly cited.

Imaging Modalities

Radiography

Since radiography is a quick and easy modality for the general evaluation of the abdomen, supine anteroposterior (AP) view is considered as the first examination for neonates and infants with GI problems. The infantogram covering the chest and abdomen includes the entire GI tract from the esophagus to the rectum in young patients. According to the patient's condition, additional views such as the left lateral decubitus view or the cross-table lateral view can be considered as the next step with a better demonstration of intraperitoneal free air, air-fluid levels, and rectal gas. In addition, pneumatosis intestinalis and ascites were observed on radiographs.

It is important to evaluate the bowel gas patterns on radiography. Soon after birth, the neonate swallows air, and the air progresses to the stomach. Bowel gas is normally seen in the duodenum at 1 hour after birth, the proximal small bowel at 3 hours, the entire small bowel at 12 hours, and the rectum by the first 24 hours. Sometimes, it may be challenging to differentiate small bowel gas from colon gas because the colonic haustra are immature in these young patients. In such cases, a long linear air-fluid level in the

colon seen in the cross-table lateral view might be helpful. Bowel dilatation is defined when the diameter of the bowel is larger than the interpedicular width of the L2 vertebra. We can suspect a high-level GI obstruction when there are three or fewer dilated bowel loops and a low-level when there are more than three.

Fluoroscopy

Appropriate collimation, the pause and pulse technique, and the last image hold technique are crucial for minimizing radiation exposure during fluoroscopic examinations [1,2].

For abnormalities in the upper GI tract, from the esophagus to the proximal small bowel, an upper gastrointestinal (UGI) series is performed with the ingestion of barium or water-soluble contrast media. For the lower GI tract, from the distal small bowel to the rectum, a contrast enema study is performed with retrograde instillation of contrast media through a rectal catheter.

Ultrasonography

As ultrasonography (US) enables real-time and bedside examination without radiation exposure, it has been more frequently used for GI evaluation in neonates and infants. However, it is not always accepted as a routine examination for neonatal GI emergencies because it is highly dependent on the operator's skill and can be potentially limited by the intervening bowel gas [1]. Exceptionally in hypertrophic pyloric stenosis (HPS), US is the gold standard for diagnosis [3].

CT and MRI

CT and MRI are selectively used for the evaluation of GI emergencies in neonates and infants and are usually reserved for complicated cases. The potential requirement for sedation, radiation hazards of CT, and relatively long examination time for MRI are significant disadvantages.

Upper Gastrointestinal Emergency

Esophageal Atresia and Tracheoesophageal Fistula

Esophageal atresia (EA), the most common congenital esophageal anomaly, shows a wide spectrum related to tracheoesophageal fistula (TEF), of which the most common type is EA with a distal TEF (85%) [4]. In addition, EA and TEF can be associated with other congenital anomalies involving musculoskeletal, GI, cardiovascular, and genitourinary systems, with a VACTERL association

(Vertebral, Anorectal, Cardiovascular, Tracheal, Esophageal, Renal, and Limb) [5]. Prenatally, polyhydramnios and the absence of a gastric bubble may suggest EA. After birth, neonates typically present with excessive drooling, regurgitation, and respiratory distress during feeding. When EA is suspected, a chest AP radiograph taken with a feeding tube is recommended, and the rolled-up feeding tube in the proximal pouch of the atretic esophagus is diagnostic (Fig. 1A). The presence of distal TEF can be attributed to the presence of stomach and distal bowel gas.

The H-type TEF differs from other types of TEF in that there is no EA. The term "H-type" comes from the morphologic features of the trachea, a traversing fistula, and the esophagus shown in the esophagogram [6]. Most patients present with choking or cyanotic spells during feeding in the neonatal period and recurrent pneumonia in the later period. For diagnosis, esophagography was performed in the prone position with gradual injection of the contrast material through a nasogastric tube, while slowly pulling the tube from the distal to the proximal esophagus is helpful [7]. The fistulas are usually small, and most have a cephalad course from the proximal esophagus to the trachea (Fig. 1B).

Hypertrophic Pyloric Stenosis

The pylorus is composed of a thicker inner circular muscle layer and a thinner outer longitudinal muscle layer. In HPS, marked hypertrophy and hyperplasia of the circular muscle, and occasionally the longitudinal, is noted in a focal or diffuse pattern [8]. In addition, inflammatory and degenerative changes in the ganglion cells of the myenteric plexus are also observed. Therefore, a thickened elongated pylorus is unable to relax, causing gastric outlet obstruction. The typical symptom is a projectile, nonbilious vomiting presenting at 3–12 weeks of age, which requires surgical intervention [1,9].

US is the gold standard for the diagnosis of HPS, with nearly 100% sensitivity [10]. The ultrasonographic diagnostic criteria are a hypertrophied pyloric muscle, persistently equal to or greater than 3 mm in thickness, and an elongated pyloric canal, equal to or greater than 15 mm in length (Fig. 2A) [9,11,12]. In abdominal radiography, a markedly distended stomach with peristaltic waves and minimal distal gas are characteristic (Fig. 2B).

Duodenal Atresia

Duodenal atresia, the most common cause of neonatal

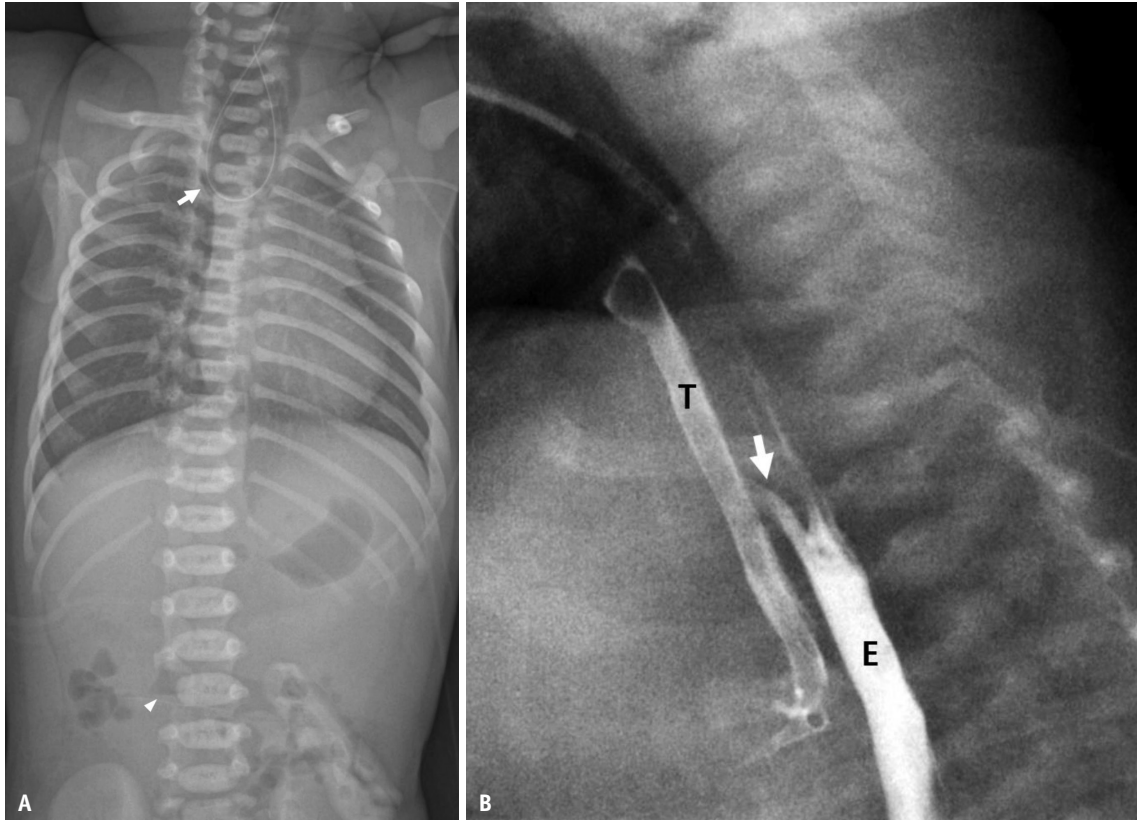


Fig. 1. Esophageal atresia.

A. Infantogram of a newborn shows the feeding tube curled (arrow) within the air-filled blind pouch of the upper esophagus. Air bubbles in the stomach and distal bowel suggest distal TEF. In addition, the right pedicle of the L4 vertebra is absent (arrowhead). **B.** Esophagogram taken with careful contrast injection through a nasogastric tube in a 25-day-old male neonate shows a fistula (arrow) with a cephalad course from the proximal esophagus (E) to the trachea (T), consistent with H-type TEF. TEF = tracheoesophageal fistula

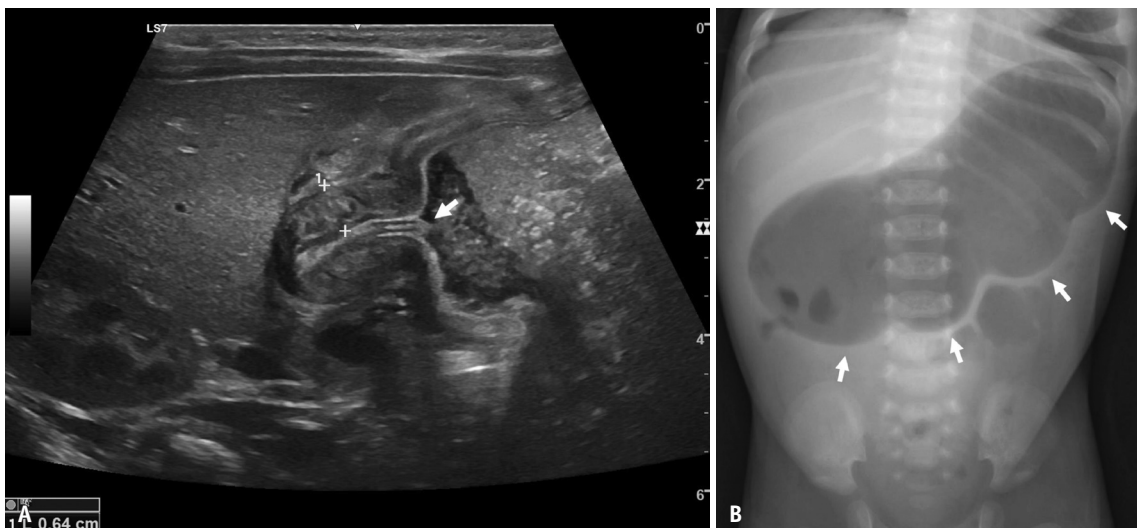


Fig. 2. Hypertrophic pyloric stenosis.

A. Upper abdominal transverse sonogram with a 6–15 MHz linear transducer in a 1-month-old male infant with projectile vomiting shows an increased thickness of the single muscular layer of the pylorus of 6.4 mm, which is greater than 3 mm, suggesting hypertrophic pyloric stenosis. A prolapsed and hypertrophied echogenic pyloric mucosa (arrow) protruding into the gastric antrum, known as the “antral nipple” sign, is also shown. **B.** Correlative supine anteroposterior abdominal radiograph from the same patient shows a markedly distended stomach with peristaltic waves seen on the greater curvature (arrows), known as the “caterpillar” sign, and minimal distal bowel gas.

proximal bowel obstruction, occurs in one in every 5000 to 10000 births, and the typical symptom is bilious vomiting within the first 24 hours of life [13]. It is believed to result from the embryologic failure of recanalization of the duodenal lumen [1]. In approximately 50% of patients, duodenal atresia is associated with other anomalies, including Down syndrome, annular pancreas, malrotation, renal anomaly, and congenital heart disease [14]. The annular pancreas results from the incomplete rotation of the ventral pancreatic primordium, which remains anterior to the duodenum. This ring of pancreatic tissue encircles the duodenum by fusion with the dorsal pancreatic primordium, causing partial or complete duodenal obstruction (Fig. 3B) [15].

The characteristic abdominal radiographic findings are marked distension of the stomach and proximal duodenum, known as the “double-bubble” sign, and the absence of distal air (Fig. 3A). The double bubble of the dilated stomach and duodenum is also detectable in prenatal US with concomitant polyhydramnios.

Malrotation and Midgut Volvulus

During development, the midgut normally rotates at 270° counterclockwise. Malrotation encompasses the spectrum of abnormalities of normal bowel rotation, including failure of rotation, incomplete rotation, reverse rotation, and reverse nonrotation. In addition, abnormal fixation of either the duodenojejunal or cecal poles potentially causes bowel obstruction. The clinical presentations vary from asymptomatic to those requiring emergency surgery, such as acute bilious vomiting in the midgut volvulus, depending upon the complications and associated malformations

[14,16]. Approximately 80% of symptomatic patients manifest in the neonatal period, mostly in the first week of life [16], as a result of proximal bowel obstruction from extrinsic peritoneal bands, midgut volvulus, or both.

In patients with malrotation without obstruction or volvulus, abdominal radiographs may show an unusual distribution of stool, which is crowded in the mid to left abdomen and absent in the right lower quadrant abdomen. The UGI series is the gold standard for the diagnosis of malrotation [17], showing an abnormally positioned duodenojejunal junction (Fig. 4A), which is a pathognomonic finding. The normal position of the duodenojejunal junction is left to the left pedicle of the vertebral body at the duodenal bulb level and posterior (retroperitoneal) on the lateral view. US has an emerging role in the diagnosis of malrotation by evaluating the relative positions of the superior mesenteric artery (SMA) and superior mesenteric vein (SMV), where the SMV normally lies to the right and anterior (9–12 o’clock position) to the SMA (Fig. 4B) [13]. When there is a reversal of this relative position, malrotation is suspected, with a sensitivity of 44%–87% and a specificity of 98% (Fig. 4C) [16,18].

In midgut volvulus, abdominal radiographs may be false negative in the early stages, and sometimes it might be too late when obviously abnormal findings including distension of the stomach and duodenum with the absence of distal air are seen. The UGI series shows a dilated duodenum with abrupt narrowing and “corkscrew” appearance of a twisted distal bowel loop (Fig. 4D). In the US, a dilated third portion of the duodenum in the abnormal right position and twisted mesenteric vessels, known as a “whirlpool” sign, is seen (Fig. 4E) [19].

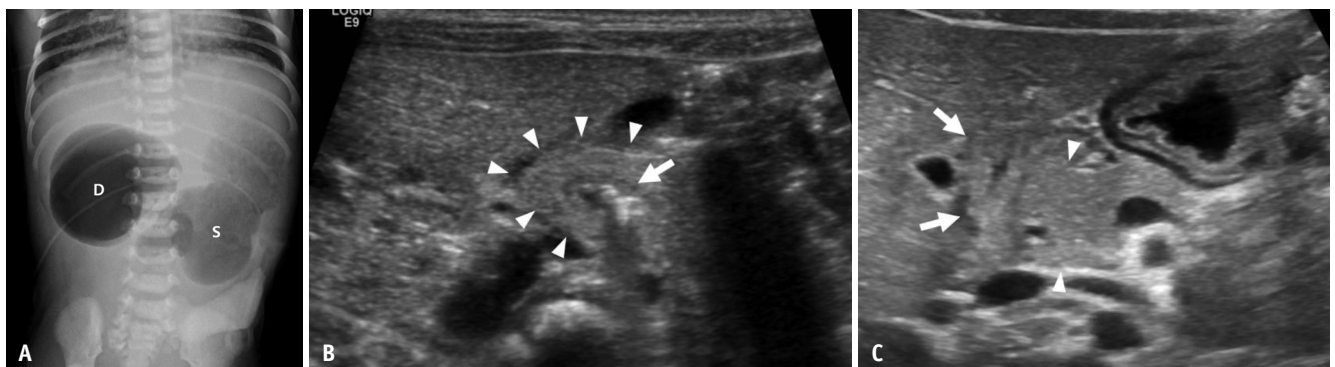


Fig. 3. Duodenal atresia and annular pancreas.

A. Supine anteroposterior abdominal radiograph of a newborn with bilious vomiting shows gaseous distension of stomach (S) and duodenum (D), the classic “double-bubble” sign, suggesting duodenal atresia. **B.** Upper mid abdominal transverse sonogram of a neonate with bilious vomiting shows the normal pancreatic tissue (arrowheads) encircling the duodenum (arrow), suggesting the annular pancreas with partial duodenal obstruction. **C.** Normal position of the duodenum and pancreas is shown; duodenum descending part (arrows) is located at the right side of the pancreas head (arrowheads).

Lower Gastrointestinal Emergency

Jejunioileal Atresia

Jejunioileal atresia is thought to occur from a late in utero ischemic insult to the mesentery, unlike duodenal atresia, which is the result of recanalization failure [14]. It is

subdivided into five patterns in the Grosfeld classification: type I, mucosal web; type II, fibrous cord; type IIIa, mesenteric defect with discontinuity in the bowel; type IIIb, a wide mesenteric defect with long segmental atresia (“apple-peel”); and type IV, multiple atresias [20].

The clinical presentations and imaging findings vary

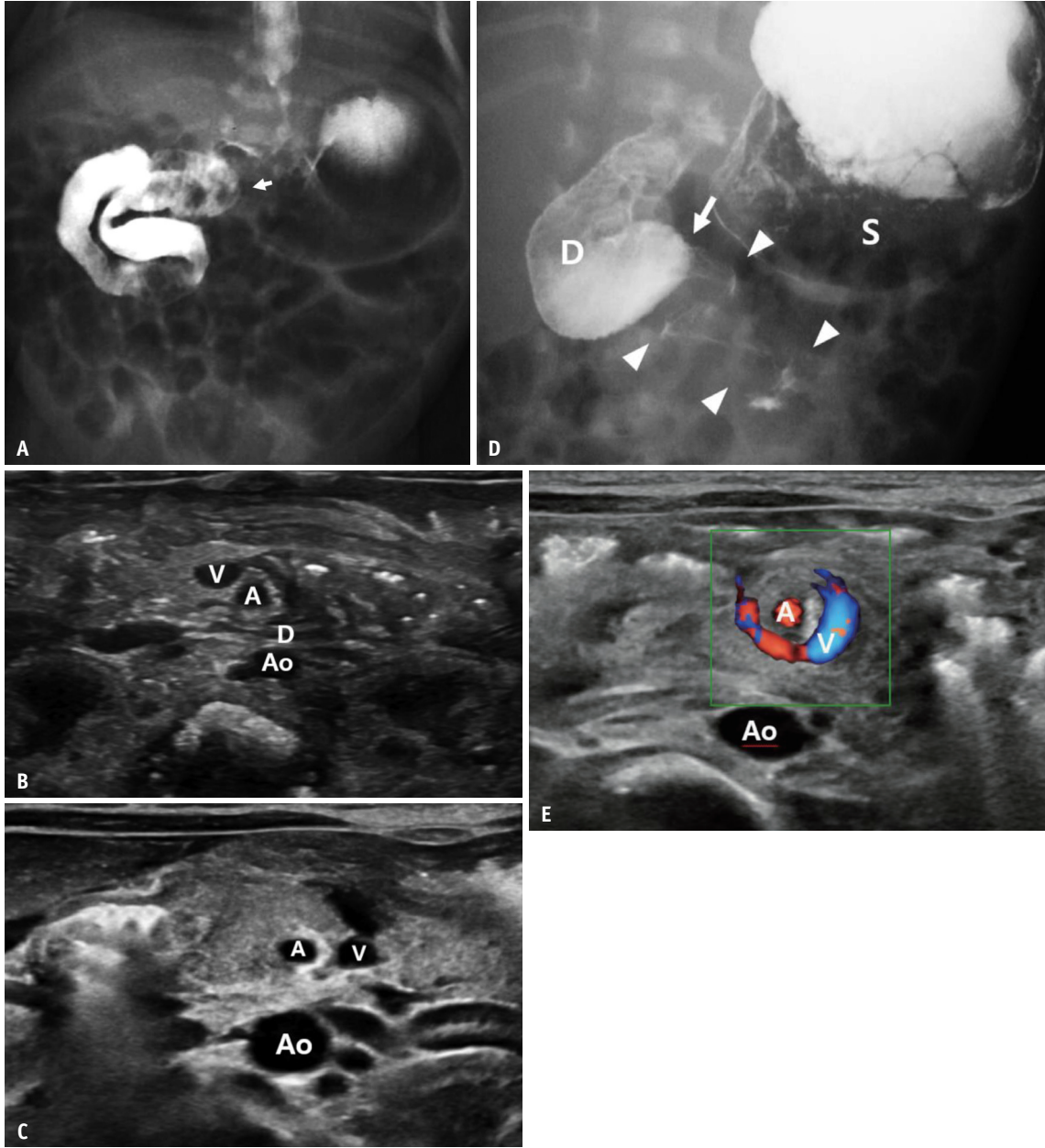


Fig. 4. Malrotation and midgut volvulus.

A. UGI series of a 3-day-old male neonate shows abnormal duodenojejunal junction (arrow) that failed to cross the left pedicle of the vertebral body. **B.** The normal relationship of the SMA (A) and SMV (V), that SMV is located at the right and anterior to the SMA. The collapsed duodenum 3rd portion (D) is located between the SMA and the Ao. **C.** Upper mid abdominal transverse sonogram of the patient with malrotation shows an inversion of the normal relationship, that SMV (V) is located at the left to the SMA (A). **D.** UGI series of a 13-day-old male neonate with bilious vomiting shows distended stomach (S) and duodenum (D), and an abrupt luminal narrowing (arrow) and “corkscrew” appearance (arrowheads) of spiraling distal bowel loops, typical findings of the midgut volvulus. **E.** Correlative transverse color Doppler sonogram from the same patient in (D) shows clockwise twisting of the SMV (V) around the SMA (A), the center of the volvulus. Ao = aorta, SMA = superior mesenteric artery, SMV = superior mesenteric vein, UGI = upper gastrointestinal

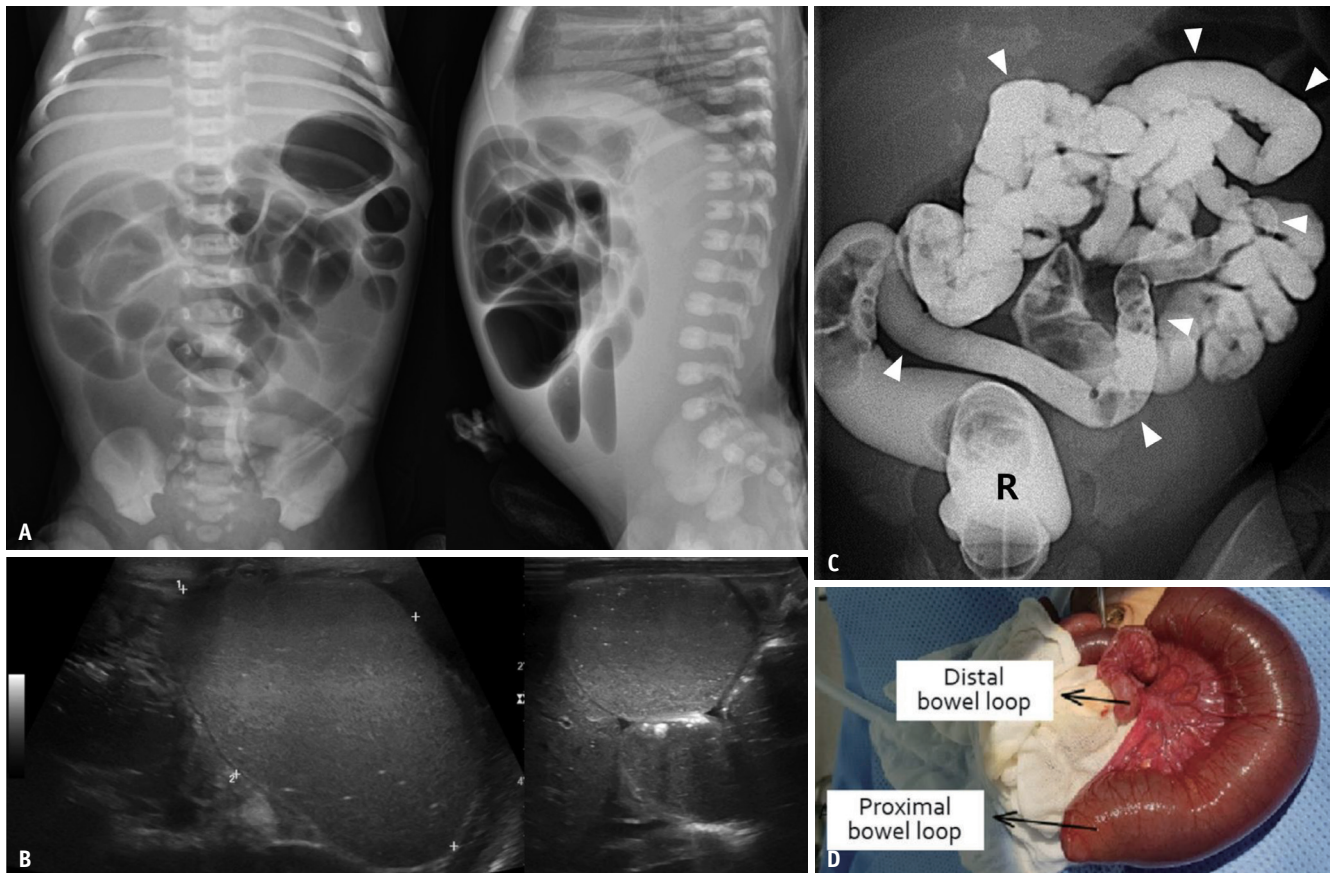


Fig. 5. Ileal atresia.

A. Infantogram and supine cross-table lateral view of a 2-day-old neonate show multiple distended small bowel loops with invisible rectal gas, suggesting lower intestinal obstruction. **B.** Abdominal transverse sonograms show markedly distended proximal ileal loops. **C.** Water-soluble contrast enema reveals an unused small-caliber colon, a microcolon (arrowheads), with normal-caliber rectum (R). **D.** In surgery, mid-ileal atresia with a mesenteric gap defect (type IIIa) was found between the markedly distended proximal ileum and the small distal ileum.

depending upon the level of obstruction and the timing of an in utero ischemic insult [14,21]. Abdominal radiographs can suggest the level of obstruction by revealing distended bowel loops proximal to the point of obstruction (Fig. 5A). The more proximal the obstruction is, the fewer the dilated small bowel loops and the less the abdominal distension. In distal small bowel atresia, water-soluble contrast enema reveals an unused microcolon (Fig. 5C), which is also beneficial for the evaluation of coexisting colonic atresia and the potential identification of the level of obstruction [1].

Meconium Ileus

Meconium ileus is a secondary obstruction of the terminal ileum by inspissated meconium due to intestinal and pancreatic dysfunction [22]. In 10%–20% of patients with cystic fibrosis, meconium ileus is the initial clinical presentation, and about 90% of patients with meconium ileus will eventually be diagnosed with cystic fibrosis [22,23].

Abdominal radiography reveals abdominal distension and multiple dilated bowel loops, consistent with distal small bowel obstruction (Fig. 6A). A “soap-bubble” appearance of the meconium admixed with air (Neuhauser sign) in the right lower quadrant abdomen on radiographs [1] and echogenic meconium in the dilated ileum on US are characteristic findings (Fig. 6B), distinct from other distal small bowel obstruction such as ileal atresia.

In uncomplicated meconium ileus, a water-soluble contrast enema using hyperosmolar agents is used for the diagnosis and treatment at the same time and may reveal an unused microcolon and multiple ovoid or round filling defects of meconium pellets in the terminal ileum (Fig. 6C) [1].

Meconium Plug Syndrome

In meconium plug syndrome, also known as functional immaturity of the colon, desiccated meconium plugs cause

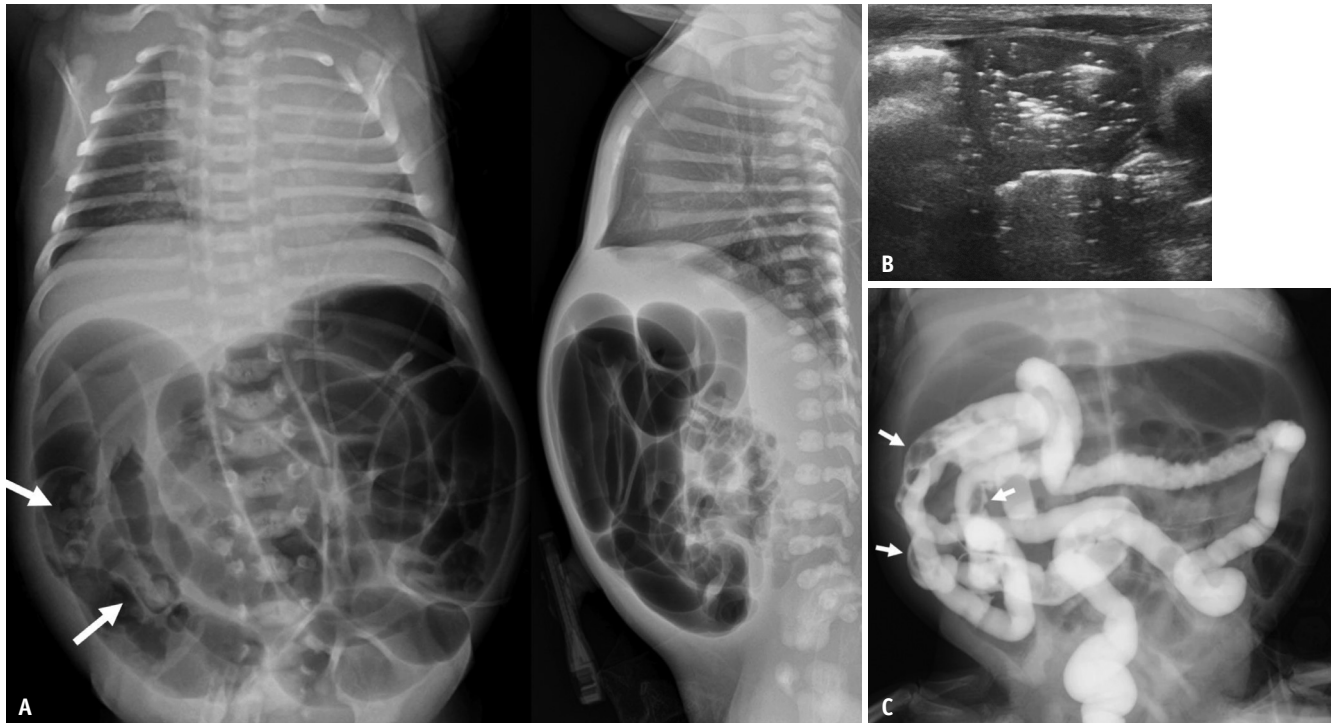


Fig. 6. Meconium ileus.

A. Infantogram and supine cross-table lateral view of a full-term newborn show multiple distended bowel loops with the absence of colorectal gas, suggesting distal small bowel obstruction. Characteristically, there are several radiopaque lesions in the right-side bowel loops (arrows), suggesting meconium pellets. **B.** Correlative abdominal sonogram from the same patient shows distended distal ileum filled with mixed echogenic content and multifocal echogenic foci suggesting admixed air or calcification in meconium. **C.** In water-soluble contrast enema, the microcolon is demonstrated with multiple filling defects (arrows) in the distal small bowel, suggesting meconium pellets.

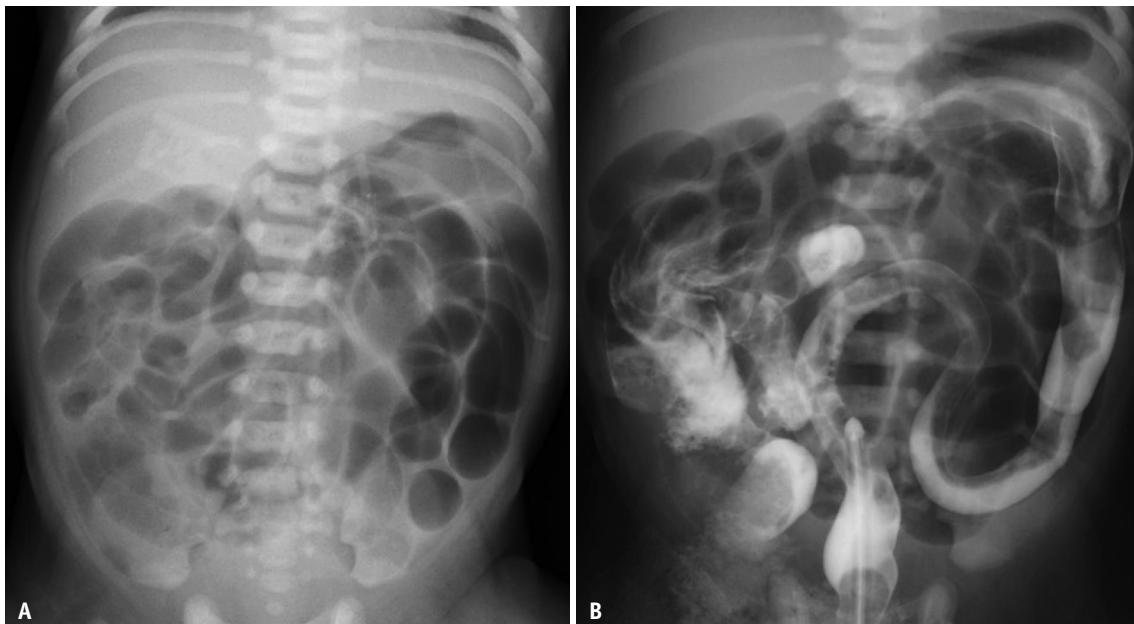


Fig. 7. Meconium plug syndrome.

A. Supine anteroposterior abdominal radiograph of a newborn (gestational age 37 + 1 weeks) from a diabetic mother shows diffuse distended small bowel loops without visible rectal gas suggesting distal bowel obstruction. **B.** In water-soluble contrast enema of the same patient, a long segment of filling defect in the small-caliber sigmoid to descending, transverse, and ascending colon is noted, suggesting meconium plug syndrome.

functional distal bowel obstruction. It is relatively common in newborns (1 in 500 live births), mainly in premature babies, and is thought to occur from an ineffective peristalsis due to an immature myenteric nervous system and excessive water absorption [24].

Premature newborns with very low or extremely low birth weight and newborns of diabetic mothers are at a higher risk, and the affected baby fails to pass meconium and develops abdominal distension [25].

Abdominal radiography shows a distal bowel obstruction pattern (Fig. 7A). Water-soluble contrast enema has both a diagnostic and therapeutic role and shows a long segment of filling defect suggesting meconium in the colon (Fig. 7B). The colon, especially the left, shows a small caliber resembling a microcolon, but the rectum is typically of normal diameter. Most cases improve after meconium passage without surgical intervention, but close monitoring is required to rule out Hirschsprung disease [26].

Meconium Peritonitis

Intrauterine bowel perforation and leakage of sterile meconium into the peritoneal cavity cause aseptic chemical peritonitis with intense inflammation, dense fibrosis, and dystrophic calcifications in hours to days. The common underlying causes are small bowel atresia and meconium ileus [27]. In generalized meconium peritonitis, diffuse dystrophic peritoneal calcifications are seen in the radiographs (Fig. 8A), and highly echogenic foci suggesting calcifications with variable acoustic shadowing on the peritoneal surface and diffuse heterogeneously echogenic ascites known as a “snowstorm appearance” are characteristic US findings [27]. In the localized cystic type, the spilled meconium becomes walled-off due to fibrous adhesions and is seen as a complex cystic mass containing echogenic meconium with hyperechoic wall calcifications in the US (Fig. 8B) [13].

Hirschsprung Disease

Hirschsprung disease occurs in one in every 5000 live births, and 80% of patients present in the newborn period [26]. Associations with other conditions have been reported in up to 30% of patients, of which Down syndrome is the most common [28]. It is considered a neurocristopathy, characterized by the failure of normal migration of the vagal neural crest cells in the intestine that results in the congenital absence of parasympathetic neuronal ganglion cells, failure of relaxation, and subsequent functional

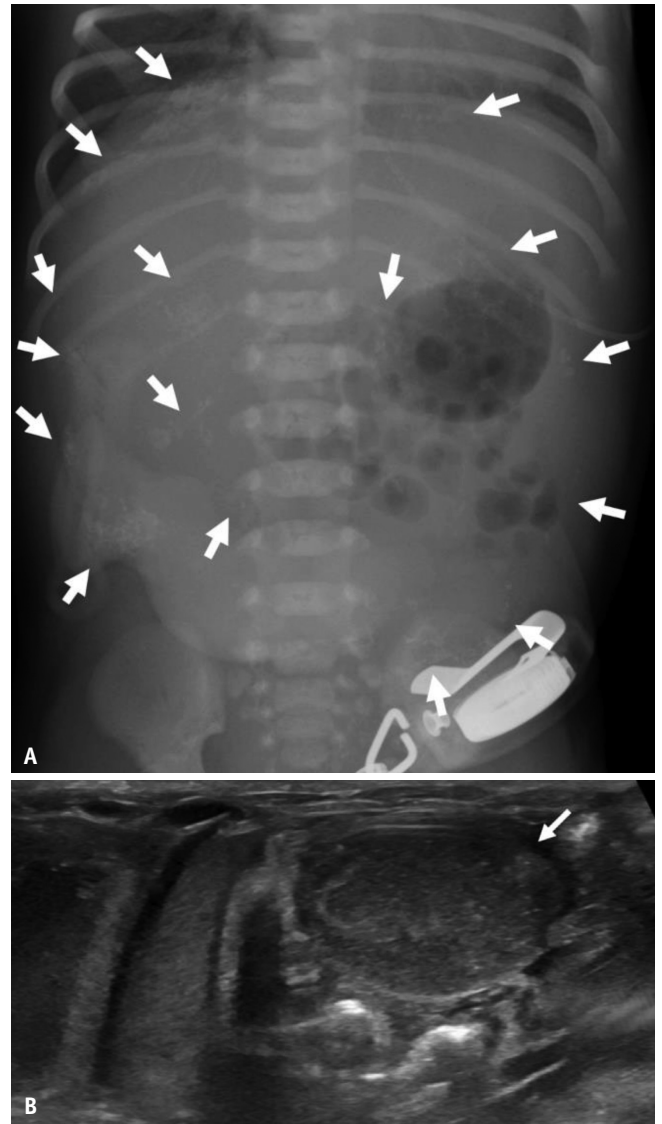


Fig. 8. Meconium peritonitis.
A. Supine anteroposterior abdominal radiograph of a newborn with generalized meconium peritonitis shows multiple stippled calcifications throughout the abdomen (arrows). **B.** Abdominal sonogram of a 6-day-old neonate with a localized cystic type of meconium peritonitis shows a well-defined cystic mass (arrow) with heterogeneous internal echogenicity in the left mid abdomen suggesting a meconium pseudocyst.

obstruction [26]. The aganglionic segment extends retrograde from the distal rectum in variable length, and the transition between the aganglionic segment and normal bowel can occur at any point, most commonly in the rectosigmoid junction (short-segment disease, about 80%–90%) [26]. In short-segment disease, the male-to-female ratio is 4:1 [1,26].

The clinical presentations in neonates are delayed or failed meconium passage in the first 48 hours after birth,

abdominal distension, and bilious vomiting. In addition, the disease can manifest in childhood with prolonged constipation, abdominal distension, and failure to thrive.

The confirmative diagnosis of Hirschsprung disease is made by histopathologic demonstration of aganglionosis [26]. Imaging studies can show the extent of the disease and therefore suggest a proper biopsy site. Abdominal radiographs show distal bowel obstruction patterns (Fig. 9A), but small rectal gas may be visible in prone cross table lateral view, unlike other distal bowel atresias [26].

Contrast enema is performed without bowel preparation and rectal ballooning to avoid inappropriate stimulation of the rectum, and a funnel-shaped transition zone between the distended proximal bowel filled with stool and a small-caliber distal aganglionic segment is diagnostic (Fig. 9B) [26]. A reversed rectosigmoid index of < 0.9 is typical in short-segment disease [29]. In addition, a 24-hour delayed image is helpful for evaluating the evacuation delay.

Total colonic aganglionosis involves the entire colon and distal small bowel and may be familial without sexual



Fig. 9. Hirschsprung disease.

A. Infantogram and supine cross-table lateral view of a 1-day-old neonate show markedly distended rectosigmoid junction without visible distal rectal gas. **B.** Contrast enema performed on the same patient with **(A)** shows distended rectosigmoid junction with funnel-shaped transition zone (arrows) at the upper rectum. **C.** Contrast enema of a 15-day-old girl with total colonic aganglionosis shows a normal caliber colon with rounded hepatic and splenic flexures (arrows), configurating a question-mark-shaped colon. **D.** Correlative 24-hours-delay abdominal radiograph from the same patient in **(C)** shows significant amount of contrast material remained in the colon indicating delayed passage of contrast.

predominance. Imaging findings are variable, including a normal caliber colon, a microcolon, and a question-mark-shaped colon that is foreshortened with rounded flexures (Fig. 9C) [25,30].

Anorectal Malformation

Anorectal malformation (ARM) resulting from an abnormal separation of the hindgut from the urogenital tract in embryonic life, encompasses a broad spectrum of congenital abnormalities in the anus, distal rectum, and urogenital tract [26]. It occurs in one in every 5000 live births, and

about one-third of the patients present with an isolated anomaly, and the other two-thirds are associated with other congenital anomalies, especially as a part of the VACTERL anomaly [31].

ARMs mostly appear as an imperforate anus and blind end pouch of the hindgut with or without a fistula and are classified into three types of low, intermediate, and high according to the relative position of the rectal pouch and puborectal sling, and the type and location of fistula [32].

The role of imaging in ARM is crucial for demonstrating the accurate anatomy, including the location of the distal

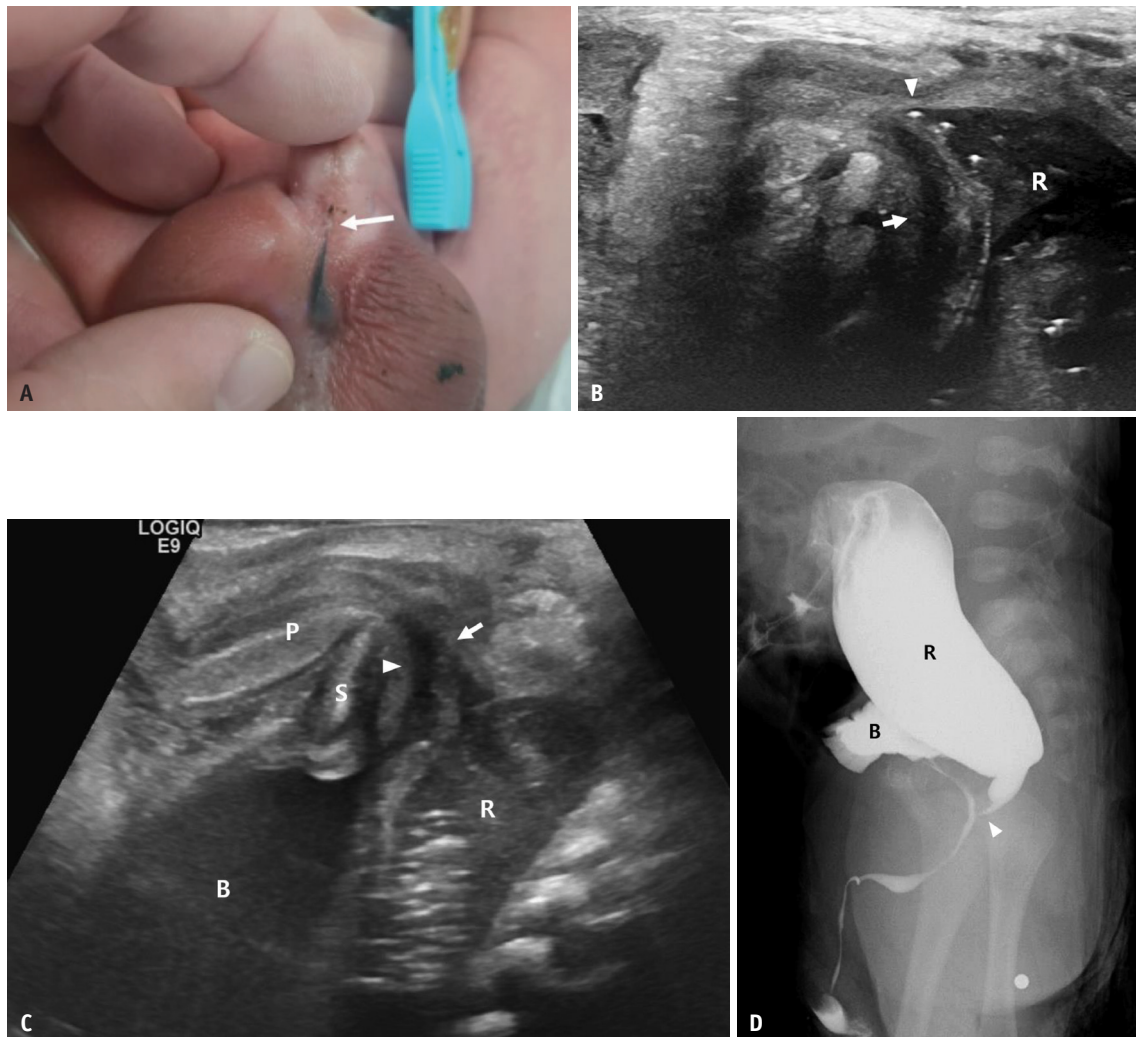


Fig. 10. Anorectal malformation.

A. Physical examination of a neonate with a low type anorectal malformation and imperforate anus reveals meconium tracking along the fistula with an opening at the proximal penile shaft (arrow). **B.** Longitudinal transperineal sonogram with a 6–15 MHz linear probe in the same patient in **(A)** shows the beaking appearance (arrowhead) of the blind end pouch of the distal rectum (R), posterior to the urethra (arrow). **C.** Longitudinal transperineal sonogram with a 6–15 MHz linear probe of a full-term baby with a high-type anorectal malformation shows the bladder (B), rectum (R), penile root (P), and symphysis pubis (S). The distal end of the rectum shows the beaking appearance toward the urethra (arrowhead) and forms a rectourethral fistula (arrow). **D.** Correlative distal loopogram through the distal colon from the same patient in **(C)** shows simultaneous contrast filling in the rectum (R) and urinary bladder (B) together with rectourethral fistula (arrowhead), consistent with a high-type anorectal malformation.

rectal pouch, possible rectourogenital fistulae, and other associated anomalies [33]. The initial imaging work-up in the first two days of life includes thorax, spine, and pelvis radiography and cardiac, transperineal, abdominal, pelvic, and spine US [32]. The previously used invertogram is no longer recommended because of its inaccuracy [32,34]. High-resolution transperineal US is an excellent method to elucidate the location of the distal rectal pouch and possible rectourogenital fistulae (Fig. 10B, D) [33-35]. MRI is also used for a detailed evaluation of the internal

anatomy and other associated malformations. Voiding cystourethrography (VCUG) is recommended for all ARM patients with any genitourinary anomalies and suspicious recurrent fistulae (Fig. 10C) [32,36].

Necrotizing Enterocolitis

Necrotizing enterocolitis (NEC) is the most common surgical emergency with higher morbidity and mortality than any other surgical GI condition in neonates [37]. Most patients are premature babies with low birth weight

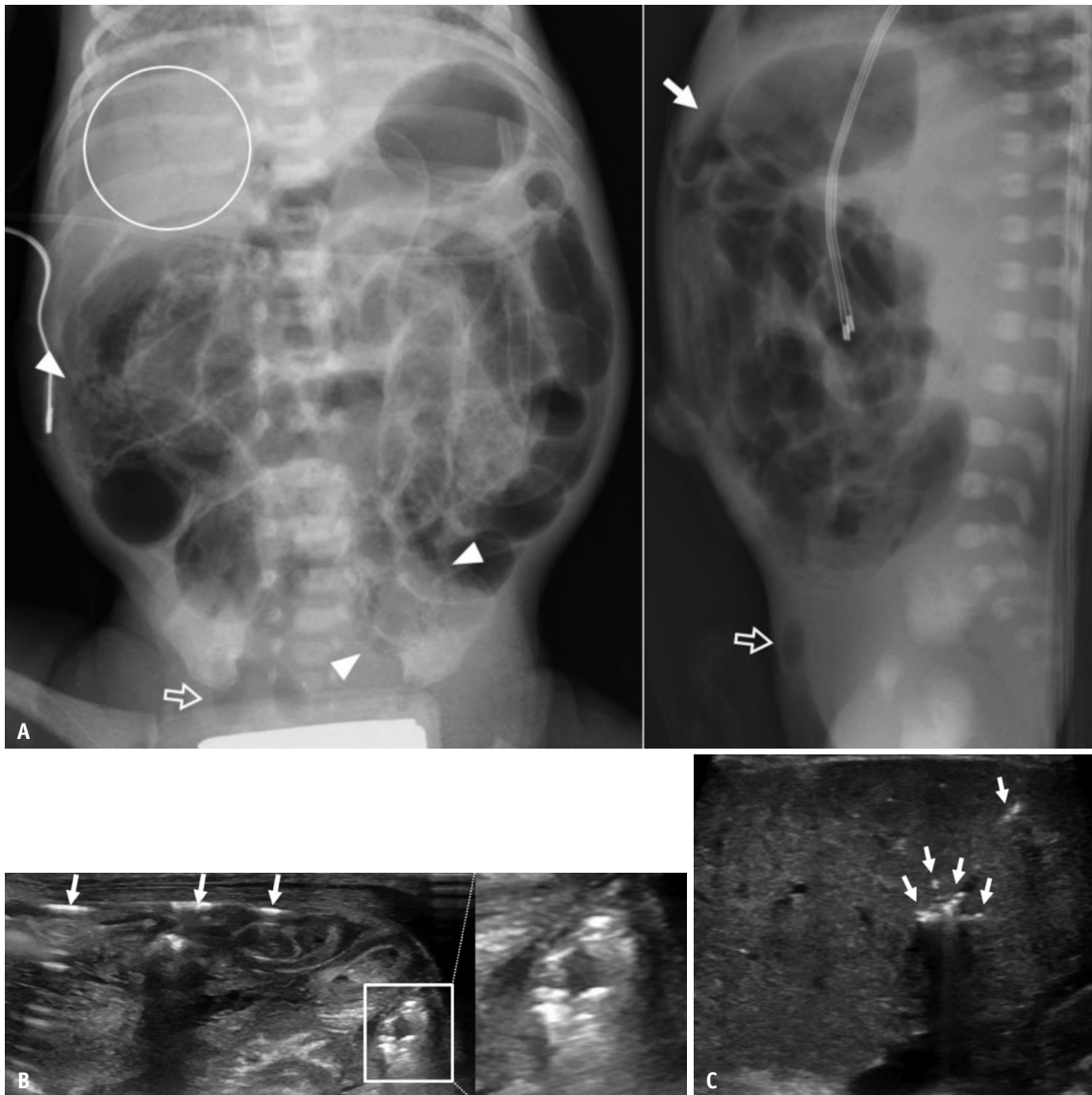


Fig. 11. Necrotizing enterocolitis.
A. Supine anteroposterior and supine cross-table lateral abdominal radiographs of a 7-day-old preterm baby show diffuse small bowel distension, peritoneal free air (arrow), radiolucent branching density in the liver suggesting portal venous gas (circle), multifocal bubbly air density of pneumatosis (arrowheads) suggesting necrotizing enterocolitis with perforation. In addition, air is visible in the patent right inguinal canal (empty arrows) in this patient. **B.** Transverse abdominal sonogram of a 9-day-old preterm baby shows intramural air in the descending colon (box and magnified image on the right) and peritoneal free air (arrows) suggesting bowel perforation. **C.** Transverse sonogram of the liver of a 4-day old preterm baby shows multiple hyperechoic foci (arrows), some with posterior acoustic shadowing, consistent with portal venous gas.

(especially 500–750 g), and only 7%–13% are full-term infants, showing an inversely proportional incidence to gestational age and birth weight [37]. The etiology is still not perfectly understood but is considered to be multifactorial, including ischemia, pathogenic intestinal microbiota, and enteral feeding in a susceptible host leading to bowel injury and an inflammatory reaction [26]. The most critical risk factors for NEC are prematurity and enteral feeding, accounting for approximately 90% of cases [26,37].

The clinical presentation varies from nonspecific findings of physiological instability including bradycardia, lethargy, and temperature instability to more specific findings such as abdominal distension, abdominal tenderness, bloody stools, vomiting, and disseminated intravascular coagulation, reflecting the severity and stage of the disease [26,37].

Interpretation of imaging studies along with clinical presentation is important in diagnosing NEC and staging the severity according to the modified Bell staging criteria [38]. In stage I (suggestive of NEC), the findings are nonspecific, with a normal bowel gas pattern or mild ileus. In stage II (definitive NEC), specific pneumatosis intestinalis and portal venous gas are detectable, and ascites is seen in progressed cases (IIB). In stage III (advanced NEC), more prominent findings of bowel necrosis and perforation are

observed. The supine AP and cross-table lateral views are the cornerstones of imaging for NEC and reveal any of the followings: ileus, pneumatosis intestinalis, portal venous gas, pneumoperitoneum, ascites, and fixed bowel loop dilatation (Fig. 11A) [39]. Pneumatosis intestinalis and portal venous gas are pathognomonic for NEC, but often temporary findings, and pneumatosis intestinalis is more frequently noted when the baby has been fed [37,40].

US has an emerging role in the real-time evaluation of bowel peristalsis, ascites (even in small amount, free fluid or complicated), bowel wall thickness, perfusion of the bowel, intramural air, and portal venous gas (Fig. 11B, C).

Intussusception

Intussusception is the invagination of the intestine [41,42]. The intussusceptum, a more proximal loop, invaginates into the intussusciens, which is the more distal recipient part. It is the most common cause of acute abdomen in infants and usually occurs between 3 months and 3 years of age, most commonly between 6 months and 1 year [29,41-43].

Most cases are ileocolic and idiopathic, although hypertrophic mesenteric lymph nodes are commonly found, and about 10% have true pathological lead points such as

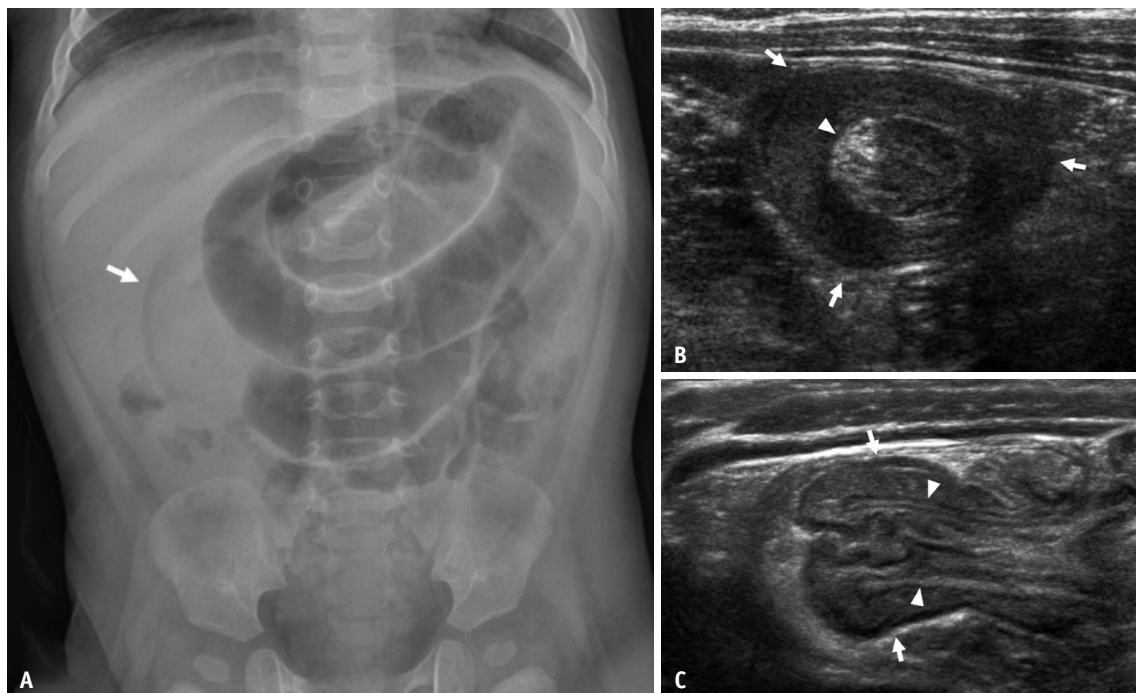


Fig. 12. Intussusception.

A. Supine anteroposterior abdominal radiograph of an 11-month-old infant shows small bowel obstruction and soft tissue mass opacity with a “crescent” sign (arrow) in the right upper abdomen. **B, C.** Transverse sonogram (**B**) in the same patient shows the target sign (arrows) of intussusception with entrapped echogenic mesenteric fat (arrowhead) and the longitudinal sonogram (**C**) shows invaginated intussusceptum (arrowheads) into the intussusciens (arrows) (bowel-within-bowel appearance).

a focal mass or diffuse bowel wall abnormalities including Meckel diverticulum, duplication cysts, polyps, lymphoma, Henoch-Schönlein purpura, and parasitic infestations, especially in the less affected age group [29,41,42]. The classic clinical presentations are colicky abdominal pain, severe cyclic irritability with pulling up the legs [42], vomiting, and currant jelly stools with a palpable abdominal mass.

Correct and timely diagnosis is important for preventing bowel necrosis and perforation, but only about 50% of the patients can be diagnosed clinically; therefore, imaging plays a key role [42]. Plain abdominal radiographs have a low sensitivity (45%–62%) and specificity (up to 85%) for intussusception [41,42,44,45]. As most cases are of the ileocolic type, the positive radiographic findings are a soft tissue mass in the right mid or upper abdomen, a paucity of gas in the ascending colon, and small bowel obstruction. The “crescent” sign, an intussusception mass outlined by gas, and the “target” sign, resulting from layered bowel loops and intervening mesenteric fat, are pathognomonic (Fig. 12A) [41,42,44]. Although a confident diagnosis of intussusception by radiographs may not be possible, the important role of radiographs is to evaluate bowel obstruction or pneumoperitoneum and to screen for other conditions [41,42].

US has almost perfect accuracy for the diagnosis of intussusception with no radiation hazard [41,46]. In addition, the evaluation of the perfusion status of the intussusceptum by Doppler US can predict the viability and reducibility of intussusception [47]. The characteristic US findings are multilayered mass-like bowel loops consisting of an infolded intussusceptum with an adjacent mesentery in edematous intussuscepti. The transverse scan of the intussusception shows the typical target or “doughnut” sign and the longitudinal scan shows a bowel-within-bowel appearance (Fig. 12B, C) [43]. US has its strength not only in the diagnosis of intussusception but also in the evaluation of lead points and prediction of prognosis. Entrapped fluid, large lead points, and decreased perfusion suggesting ischemia are known poor prognostic factors for nonoperative reduction [41,42,44,47].

Nonoperative radiologic reduction with air or normal saline enema can be attempted as the first option in non-complicated cases. Bowel perforation, peritonitis, and clinically devastating conditions are contraindications for nonoperative reduction and should be treated surgically [42]. Air enema under fluoroscopic guidance has been

reported to be superior to positive-contrast liquid enema with higher reducibility and less spillage of fecal materials if perforated [41,48]. In addition, a negative contrast of the air has superiority in the field of view and the radiation dose compared to the positive contrast of the barium [41]. Hydrostatic enema with normal saline under US guidance poses no radiation hazard and confirms the success of reduction in real time. Delayed repeat enema in several hours in partially successful cases may waive the need for surgery [49,50]. Recurrence is reported in about 10% of cases, half of which recur within 48 hours [41].

SUMMARY

The many different causes of GI emergencies in neonates and infants have overlapping clinical findings. Therefore, precise imaging is important for an accurate and timely diagnosis. Radiologists are responsible for choosing the appropriate imaging modality and considering the as low as reasonably achievable principle of radiation for young patients.

Availability of Data and Material

Data sharing does not apply to this article as no datasets were generated or analyzed during the current study.

Conflicts of Interest

The authors have no potential conflicts of interest to disclose.

Author Contributions

Conceptualization: Gayoung Choi. Data curation: Gayoung Choi, Bo-Kyung Je. Investigation: Gayoung Choi, Bo-Kyung Je. Methodology: Gayoung Choi. Project administration: Gayoung Choi, Bo-Kyung Je. Resources: all authors. Supervision: Gayoung Choi, Bo-Kyung Je. Validation: Gayoung Choi, Bo-Kyung Je. Visualization: Gayoung Choi. Writing—original draft: Gayoung Choi. Writing—review & editing: Gayoung Choi, Bo-Kyung Je.

ORCID iDs

Gayoung Choi

<https://orcid.org/0000-0002-2004-5228>

Bo-Kyung Je

<https://orcid.org/0000-0001-8335-9980>

Yu Jin Kim

<https://orcid.org/0000-0001-9230-6477>

Funding Statement

None

Acknowledgments

We thank to Chaeyoun Oh for his surgical resources.

REFERENCES

1. Stanescu AL, Liszewski MC, Lee EY, Phillips GS. Neonatal gastrointestinal emergencies: step-by-step approach. *Radiol Clin North Am* 2017;55:717-739
2. Hernanz-Schulman M, States L, Vasanawala S. *Imaging techniques*. In: Coley BD, ed. *Caffey's pediatric diagnostic imaging*, 13th ed. Philadelphia: Elsevier Saunders, 2019:761-776
3. Hiorns MP. Gastrointestinal tract imaging in children: current techniques. *Pediatr Radiol* 2011;41:42-54
4. Bax KM. *Esophageal atresia and tracheoesophageal malformations*. In: Holcomb GW, Murphy JP, Ostlie DJ, eds. *Ashcraft's pediatric surgery*, 5th ed. Philadelphia: Elsevier Saunders, 2010:345-361
5. Mann GS, Rizvi AA, Shabani AG, Rizvi A, Stafrace S. *The esophagus*. In: Stafrace S, Blickman JG, eds. *Radiological imaging of the digestive tract in infants and children*, 2nd ed. Cham: Springer, 2016:125-176
6. Ellis WD. *Congenital and neonatal abnormalities*. In: Coley BD, ed. *Caffey's pediatric diagnostic imaging*, 13th ed. Philadelphia: Elsevier Saunders, 2019:901-910
7. Harmon CM, Coran AG. *Congenital anomalies of the esophagus*. In: Coran AG, Caldamone A, Adzick NS, Krummel TM, Laberge JM, Shamberger R, eds. *Pediatric surgery*, 7th ed. Philadelphia: Elsevier Mosby, 2012:893-918
8. Hellan M, Lee T, Lerner T. Diagnosis and therapy of primary hypertrophic pyloric stenosis in adults: case report and review of literature. *J Gastrointest Surg* 2006;10:265-269
9. Hernanz-Schulman M. *Hypertrophic pyloric stenosis*. In: Coley BD, ed. *Caffey's pediatric diagnostic imaging*, 13th ed. Philadelphia: Elsevier Saunders, 2019:935-944
10. Ranells JD, Carver JD, Kirby RS. Infantile hypertrophic pyloric stenosis: epidemiology, genetics, and clinical update. *Adv Pediatr* 2011;58:195-206
11. Costa Dias S, Swinson S, Torrão H, Gonçalves L, Kurochka S, Vaz CP, et al. Hypertrophic pyloric stenosis: tips and tricks for ultrasound diagnosis. *Insights Imaging* 2012;3:247-250
12. Blumhagen JD, Maclin L, Krauter D, Rosenbaum DM, Weinberger E. Sonographic diagnosis of hypertrophic pyloric stenosis. *AJR Am J Roentgenol* 1988;150:1367-1370
13. Navarro OM, Siegel MJ. *Gastrointestinal tract*. In: Siegel MJ, ed. *Pediatric sonography*, 5th ed. Philadelphia: Wolters Kluwer, 2019:346-395
14. Hernanz-Schulman M. *Duodenum and small bowel: congenital and neonatal abnormalities*. In: Coley BD, ed. *Caffey's pediatric diagnostic imaging*, 13th ed. Philadelphia: Elsevier Saunders, 2019:953-978.
15. Applebaum H, Sydorak R. *Duodenal atresia and stenosis-annular pancreas*. In: Coran AG, Caldamone A, Adzick NS, Krummel TM, Laberge JM, Shamberger R, eds. *Pediatric surgery*, 7th ed. Philadelphia: Elsevier Mosby, 2012:1051-1057
16. Strouse PJ. Disorders of intestinal rotation and fixation ("malrotation"). *Pediatr Radiol* 2004;34:837-851
17. Sizemore AW, Rabbani KZ, Ladd A, Applegate KE. Diagnostic performance of the upper gastrointestinal series in the evaluation of children with clinically suspected malrotation. *Pediatr Radiol* 2008;38:518-528
18. Orzech N, Navarro OM, Langer JC. Is ultrasonography a good screening test for intestinal malrotation? *J Pediatr Surg* 2006;41:1005-1009
19. Pracros JP, Sann L, Genin G, Tran-Minh VA, Morin de Finfe CH, Foray P, et al. Ultrasound diagnosis of midgut volvulus: the "whirlpool" sign. *Pediatr Radiol* 1992;22:18-20
20. Grosfeld JL, Ballantine TV, Shoemaker R. Operative management of intestinal atresia and stenosis based on pathologic findings. *J Pediatr Surg* 1979;14:368-375
21. Frischer JS, Azizkhan RG. *Jejunioileal atresia and stenosis*. In: Coran AG, Caldamone A, Adzick NS, Krummel TM, Laberge JM, Shamberger R, eds. *Pediatric surgery*, 7th ed. Philadelphia: Elsevier Mosby, 2012:1059-1071
22. Chang PT, Lee EY, Restrepo R, Eisenberg RL. Gastrointestinal tract filling defects in pediatric patients. *AJR Am J Roentgenol* 2014;203:W3-W13
23. Haber HP. Cystic fibrosis in children and young adults: findings on routine abdominal sonography. *AJR Am J Roentgenol* 2007;189:89-99
24. Arca MJ, Oldham KT. *Atresia, stenosis, and other obstructions of the colon*. In: Coran AG, Caldamone A, Adzick NS, Krummel TM, Laberge JM, Shamberger R, eds. *Pediatric surgery*, 7th ed. Philadelphia: Elsevier Mosby, 2012:1247-1253
25. Siegel MJ, Coley BD. *Esophagus and gastrointestinal tract*. In: Siegel MJ, Coley BD, eds. *Pediatric imaging*. Philadelphia: Lippincott Williams & Wilkins, 2006:199-258
26. Hernanz-Schulman M. *Congenital and neonatal disorders*. In: Coley BD, ed. *Caffey's pediatric diagnostic imaging*, 13th ed. Philadelphia: Elsevier Saunders, 2019:1008-1023
27. Berrocal T, Lamas M, Gutieérrez J, Torres I, Prieto C, del Hoyo ML. Congenital anomalies of the small intestine, colon, and rectum. *Radiographics* 1999;19:1219-1236
28. Moore SW. The contribution of associated congenital anomalies in understanding Hirschsprung's disease. *Pediatr Surg Int* 2006;22:305-315
29. DiPerna S, Buonomo C. *Gastrointestinal imaging*. In: Walters M, Robertson RL, eds. *Pediatric radiology: the requisites*, 4th ed. Philadelphia: Elsevier Inc, 2016:91-117
30. Yan J, Sun J, Wu R, Tan SS, Chen Y, Peng Y, et al. Barium enema findings in total colonic aganglionosis: a single-center, retrospective study. *BMC Pediatr* 2020;20:499
31. Herman RS, Teitelbaum DH. Anorectal malformations. *Clin Perinatol* 2012;39:403-422

32. Alamo L, Meyrat BJ, Meuwly JY, Meuli RA, Gudinchet F. Anorectal malformations: finding the pathway out of the labyrinth. *Radiographics* 2013;33:491-512
33. Kim IO, Han TI, Kim WS, Yeon KM. Transperineal ultrasonography in imperforate anus: identification of the internal fistula. *J Ultrasound Med* 2000;19:211-216
34. Niedzielski JK. Invertography versus ultrasonography and distal colostography for the determination of bowel-skin distance in children with anorectal malformations. *Eur J Pediatr Surg* 2005;15:262-267
35. Choi YH, Kim IO, Cheon JE, Kim WS, Yeon KM. Imperforate anus: determination of type using transperineal ultrasonography. *Korean J Radiol* 2009;10:355-360
36. McHugh K. The role of radiology in children with anorectal anomalies; with particular emphasis on MRI. *Eur J Radiol* 1998;26:194-199
37. Sylvester KG, Liu GY, Albanese CT. *Necrotizing enterocolitis*. In: Coran AG, Caldamone A, Adzick NS, Krummel TM, Laberge JM, Shamberger R, eds. *Pediatric surgery*, 7th ed. Philadelphia: Elsevier Mosby, 2012:1187-1207
38. Kliegman RM, Walsh MC. Neonatal necrotizing enterocolitis: pathogenesis, classification, and spectrum of illness. *Curr Probl Pediatr* 1987;17:213-288
39. Morrison SC, Jacobson JM. The radiology of necrotizing enterocolitis. *Clin Perinatol* 1994;21:347-363
40. Marchildon MB, Buck BE, Abdenour G. Necrotizing enterocolitis in the unfed infant. *J Pediatr Surg* 1982;17:620-624
41. Applegate KE, Hernanz-Schulman M. *Intussusception*. In: Coley BD, ed. *Caffey's pediatric diagnostic imaging*, 13th ed, Philadelphia: Elsevier Saunders, 2019:1040-1049
42. Columbani PM, Scholz S. *Intussusception*. In: Coran AG, Caldamone A, Adzick NS, Krummel TM, Laberge JM, Shamberger R, eds. *Pediatric surgery*, 7th ed. Philadelphia: Elsevier Mosby, 2012:1093-1110
43. Cogley JR, O'Connor SC, Houshyar R, Al Dulaimy K. Emergent pediatric US: what every radiologist should know. *Radiographics* 2012;32:651-665
44. Daneman A, Alton DJ. Intussusception. Issues and controversies related to diagnosis and reduction. *Radiol Clin North Am* 1996;34:743-756
45. Hernandez JA, Swischuk LE, Angel CA. Validity of plain films in intussusception. *Emerg Radiol* 2004;10:323-326
46. Hryhorczuk AL, Strouse PJ. Validation of US as a first-line diagnostic test for assessment of pediatric ileocolic intussusception. *Pediatr Radiol* 2009;39:1075-1079
47. del-Pozo G, González-Spinola J, Gómez-Ansón B, Serrano C, Miralles M, González-deOrbe G, et al. Intussusception: trapped peritoneal fluid detected with US--relationship to reducibility and ischemia. *Radiology* 1996;201:379-383
48. Sadigh G, Zou KH, Razavi SA, Khan R, Applegate KE. Meta-analysis of air versus liquid enema for intussusception reduction in children. *AJR Am J Roentgenol* 2015;205:W542-W549
49. Gorenstein A, Raucher A, Serour F, Witzling M, Katz R. Intussusception in children: reduction with repeated, delayed air enema. *Radiology* 1998;206:721-724
50. Dahab MM, AbouZeid AA, Mohammad SA, Safoury HS. The second trial pneumatic reduction for idiopathic intussusception: therapeutic effect and hazards. *Ann Pediatr Surg* 2012;8:77-79